HHS Public Access

Author manuscript

Sci Transl Med. Author manuscript; available in PMC 2015 November 20.

Published in final edited form as:

Sci Transl Med. 2015 May 20; 7(288): 288ra79. doi:10.1126/scitranslmed.aaa5094.

The $\alpha_v\beta_1$ integrin plays a critical in vivo role in tissue fibrosis

Nilgun I. Reed[1,*], **Hyunil Jo**[2,*], **Chun Chen**[1], **Kazuyuki Tsujino**[1], **Thomas D. Arnold**[3], **William F. DeGrado**[2,‡,†], and **Dean Sheppard**[1,‡,†]

[1]Department of Medicine, University of California, San Francisco, San Francisco, CA 94143, USA

[2]Department of Pharmaceutical Chemistry, University of California, San Francisco, San Francisco, CA 94143, USA

[3]Department of Pediatrics, University of California, San Francisco, San Francisco, CA 94143, USA

Abstract

Integrins are transmembrane heterodimeric receptors that contribute to diverse biological functions and play critical roles in many human diseases. Studies using integrin subunit knockout mice and inhibitory antibodies have identified important roles for nearly every integrin heterodimer and led to the development of a number of potentially useful therapeutics. One notable exception is the $\alpha_v\beta_1$ integrin. α_v and β_1 subunits are individually present in numerous dimer pairs, making it challenging to infer specific roles for $\alpha_v\beta_1$ by genetic inactivation of individual subunits, and $\alpha_v\beta_1$ complex–specific blocking antibodies do not yet exist. We therefore developed a potent and highly specific small-molecule inhibitor of $\alpha_v\beta_1$ to probe the function of this understudied integrin. We found that $\alpha_v\beta_1$, which is highly expressed on activated fibroblasts, directly binds to the latency-associated peptide of transforming growth factor–β_1 (TGFβ_1) and mediates TGFβ_1 activation. Therapeutic delivery of this $\alpha_v\beta_1$ inhibitor attenuated bleomycin-induced pulmonary fibrosis and carbon tetrachloride–induced liver fibrosis, suggesting that drugs

‡Corresponding author. dean.sheppard@ucsf.edu (D.S.); bill.degrado@ucsf.edu (W.F.D.).
*These authors contributed equally to this work as first authors.
†These authors contributed equally to this work as senior authors.

SUPPLEMENTARY MATERIALS

www.sciencetranslationalmedicine.org/cgi/content/full/7/288/288ra79/DC1

Fig. S1. Validation of cell adhesion conditions used to determine potency and specificity of $\alpha_v\beta_1$ inhibitors.
Fig. S2. C8 and C6 adhesion assays.
Fig. S3. Adhesion of WI38 cells in low concentration of TGFβ_1 LAP.
Fig. S4. Adhesion and TGFβ activation assays in A549 and 293 cells.
Fig. S5. Original Western blot images of Fig. 2A.
Table S1. Source data for Fig. 1 (D and E).
Table S2. Source data for Fig. 2B.
Table S3. Source data for Fig. 2C.
Table S4. Source data for Fig. 2D.
Table S5. Source data for Fig. 3C.
Table S6. Source data for Fig. 3F.

Author contributions: N.I.R., H.J., D.S., and W.F.D. designed the experiments and analyzed the data. N.I.R. performed in vitro adhesion assays and in vivo fibrosis experiments. W.F.D. and H.J. designed and synthesized the inhibitors. C.C., N.I.R., and K.T. determined cellular expression of $\alpha_v\beta_1$. N.I.R. and T.D.A. performed studies of in vivo TGFβ activation. D.S. and W.F.D. directed the studies. N.I.R., H.J., T.D.A., D.S., and W.F.D. wrote the manuscript, and all authors reviewed it.

Data and materials availability: c8 can be available for research purposes through a material transfer agreement with UCSF.

based on this lead compound could be broadly useful for treatment of diseases characterized by excessive tissue fibrosis.

INTRODUCTION

Integrins are present in nearly all multicellular organisms and play a conserved role in mediating cell adhesion to fixed extracellular ligands and in the maintenance of tissue integrity (1). In invertebrates, a surprisingly small number of integrin heterodimers mediate these diverse functions (2, 3). Much has been learned about the critical in vivo functions of most members of the integrin family through the use of mice with global or conditional inactivating mutations of individual subunits (4, 5) and through the use of heterodimer-specific blocking monoclonal antibodies (6, 7). One major exception is the $\alpha_v\beta_1$ integrin. This integrin, first identified biochemically more than two decades ago (8), is composed of α and β subunits that are both present in multiple heterodimers (5 in the case of α_v and 12 in the case of β_1) (1), which has made it difficult to generate heterodimer-specific antibodies or to infer function from gene knockout studies. As a result, this integrin has been largely ignored.

We and others have shown that two members of the integrin family, $\alpha_v\beta_6$ and $\alpha_v\beta_8$, have as their principal ligands latency-associated peptides (LAPs) of the growth factors TGFβ_1-3 (transforming growth factor–β_1-3) (9–11) and that these integrins play major roles in activation of latent forms of this growth factor that are stored in the extracellular matrix in most healthy adult tissues. In mice, inactivation of both of these integrins recapitulates all of the developmental phenotypes of loss of TGFβ_1 and TGFβ3 (12). Inhibitors of each of these integrins have identified important and distinct roles for each in multiple disease models and have provided new options for therapeutically targeting TGFβ in specific contexts, thereby avoiding potentially undesirable side effects of globally inhibiting this pleiotropic growth factor (9, 13–16).

However, in contrast to development, it is clear that there are a number of important pathologic circumstances in adults where inhibition of TGFβ is therapeutically effective, but inhibition of $\alpha_v\beta_6$ and $\alpha_v\beta_8$ is not. One of these is hepatic fibrosis (17). We recently used cremediated deletion of the integrin α_v subunit in activated fibroblasts to demonstrate that loss of all α_v integrins from these cells protects mice from fibrosis in multiple organs, including the liver, and that this effect was associated with reduced tissue TGFβ signaling (17). Tissue fibroblasts can express four α_v-containing integrins, $\alpha_v\beta_1$, $\alpha_v\beta_3$, $\alpha_v\beta_5$, and $\alpha_v\beta_8$. We found that individual deletion of $\alpha_v\beta_3$, $\alpha_v\beta_5$, or $\alpha_v\beta_8$ integrin either globally or conditionally in activated fibroblasts (in the case of $\alpha_v\beta_8$ integrin) had no effect on organ fibrosis but were unable to examine any possible contributions of the $\alpha_v\beta_1$ integrin because of the lack of suitable experimental tools. Our previous results could thus have been explained either by redundancy of α_v integrins (the interpretation we favored) or by a specific role for fibroblast $\alpha_v\beta_1$ in driving fibrosis.

To begin to identify important functions for the $\alpha_v\beta_1$ integrin, we used information from the solved crystal structure of other α_v and β_1 integrins (18, 19) and from the design of other small-molecule inhibitors targeting integrins (20), to develop a potent and specific small-

molecule inhibitor of the $\alpha_v\beta_1$ integrin. We then used this inhibitor to demonstrate a previously unknown role for this integrin in activating the growth factor TGFβ and in driving tissue fibrosis in the lung and liver.

RESULTS

Design and synthesis of an $\alpha_v\beta_1$ integrin–specific inhibitor

Starting with a base compound that specifically binds to the α_v subunit in $\alpha_v\beta_3$ integrin, we looked to impart β_1 subunit–binding specificity through addition of a sulfonamidoproline moiety we had previously shown to bind to the β_1 subunit in $\alpha_2\beta_1$ integrin (Fig. 1A, blue shading), which occupies a hydrophobic pocket in the β_1 chain (20).

Because cocrystal structures are available for the ligand-binding regions of the $\alpha_v\beta_3$ and $\alpha_5\beta_1$ integrins (18, 19), we were able to construct a computational model of the $\alpha_v\beta_1$ integrin to further guide our inhibitor design (Fig. 1C). We then synthesized a small set of compounds, including the α_v-binding base compound and the β_1-binding sulfonamidoproline moiety separated by amide linkers of various lengths, and found outstanding geometric and electrostatic complementarity when these were docked to our model of the $\alpha_v\beta_1$ integrin. Potency and specificity of each compound were tested by performing cell adhesion assays with a panel of cell lines and ligands designed to isolate adhesion mediated by individual integrin heterodimers (Fig. 1D, fig. S1, and table S1). The most promising compound, c8 (Fig. 1B), is one of two compounds predicted to have the highest affinity based on its excellent fit to the modeled integrin structure. Indeed, c8 inhibited $\alpha_v\beta_1$ integrin– mediated cell adhesion to the previously identified ligand fibronectin (8), with a sub-nanomolar median inhibitory concentration (IC_{50}), but only minimally inhibited binding mediated by other related integrins up to concentrations five orders of magnitude higher (Fig. 1E and table S1). A related compound, c6, performed similarly well in binding assays (fig. S2). The remarkable specificity obtained for c8 and c6 demonstrated the effectiveness of our chimeric design strategy and provided us with novel reagents to examine $\alpha_v\beta_1$ integrin function.

Identification of widespread expression of the $\alpha_v\beta_1$ integrin on fibroblasts and a critical role for this integrin in activation of latent TGFβ by these cells

To determine the functional relevance of the $\alpha_v\beta_1$ integrin, we began by examining its possible role in the process of tissue fibrosis (12). Fibrosis is a critical contributor to many chronic diseases that eventually lead to organ failure. Despite the societal burden of fibrotic diseases, there are currently few approved therapies. As we reported for hepatic stellate cells, primary murine lung fibroblasts and human fetal and adult lung fibroblasts, as well as lung fibroblasts from patients with idiopathic pulmonary fibrosis (IPF), all clearly expressed the $\alpha_v\beta_1$ integrin as determined by immunoprecipitation (IP) of α_v, followed by Western blotting for β_1 (Fig. 2A and fig. S5). In contrast, whereas both the α_v and β_1 subunits were easily detectible in primary endothelial and epithelial cells, coimmunoprecipitation did not detect the $\alpha_v\beta_1$ heterodimer in these cells.

We and others have reported that the closely related α_v integrins $\alpha_v\beta_6$ (9) and $\alpha_v\beta_8$ (11) can each bind to an N-terminal fragment of the TGFβ_1 and TGFβ3 gene products called the

LAP, which normally forms a noncovalent complex with the active cytokine, preventing TGFβ from binding to its receptors and inducing biological effects. When mechanical force is applied to the latent complex by contraction of integrin-expressing cells, the resultant conformational change leads to release of active TGFβ$_1$ (21).Our previous work suggested that an α$_v$ integrin on fibroblasts contributed to tissue fibrosis by binding to and activating TGFβ (17). To determine whether the relevant fibroblast integrin could be α$_v$β$_1$, we performed cell adhesion assays with either primary fibroblasts, control α$_5$-deficient Chinese hamster ovary (CHO) cells or α$_5$-deficient CHO cells engineered to express the α$_v$β$_1$ integrin (8). Both fetal lung fibroblasts (WI38 cells) and α$_v$β$_1$ integrin–expressing CHO (CHO α$_v$) cells efficiently adhered to a range of concentrations of TGFβ$_1$ LAP, whereas control CHO (CHO wild-type) cells did not (Fig. 2B and table S2). This adhesion could be inhibited by c8 with a similar IC$_{50}$ as that shown for inhibition of adhesion to fibronectin (Fig. 2C and table S3). Adhesion to LAP could be inhibited by antibodies to either β$_1$ or α$_v$, but not with antibodies to either α$_v$β$_3$, α$_v$β$_5$, α$_v$β$_6$, or α$_v$β$_8$ (fig. S3). We used a coculture system to quantitatively assess TGFβ activation (22) and found that c8 potently and specifically inhibited activation of TGFβ by CHO cells engineered to express the α$_v$β$_1$ integrin and by a variety of primary murine and human lung fibroblasts, including fibroblasts from the lungs of patients with IPF, and murine hepatic stellate cells (Fig. 2D and table S4). The IC$_{50}$ for c8-mediated inhibition of TGFβ activation by these cells ranged from 0.35 to 0.50 nM, close to the IC$_{50}$ of 0.75 nM for inhibition of WI38 cell adhesion to LAP (Fig. 2C). Together, these data suggest that α$_v$β$_1$ is the principal integrin on fibroblasts responsible for adhesion to TGFβ$_1$ LAP and for activation of latent TGFβ. A biochemical association between the α$_v$β$_1$ integrin and TGFβ$_1$ LAP was previously reported on the basis of affinity chromatography (23), but this is the first evidence that contractile cells can use this integrin to activate TGFβ.

In vivo role of the α$_v$β$_1$ integrin in liver and lung fibrosis

Having established that c8 inhibits fibroblast adhesion to TGFβ$_1$ LAP and TGFβ activation by fibroblasts from multiple organs, we used this inhibitor to examine the role of α$_v$β$_1$ integrin–mediated TGFβ activation in two widely used models of pathologic tissue fibrosis: carbon tetrachloride (CCl_4)–induced hepatic fibrosis and bleomycin-induced pulmonary fibrosis. To determine whether α$_v$β$_1$ might be a promising therapeutic target, we waited until fibrosis was established in each model (21 days for CCl_4 and 14 days for bleomycin) and then began continuous subcutaneous administration of either c8 or an inactive control compound, c16. In each model, c8 caused a substantial and significant reduction in fibrosis, as measured by either total area of collagen staining or total organ hydroxyproline content (a measure of cross-linked collagen) (Fig. 3, A to F, and tables S5 and S6). These results are highly comparable to the protection we previously reported in mice with conditional deletion of all α$_v$ integrins from activated fibroblasts (17), suggesting that α$_v$β$_1$ was probably the major α$_v$ integrin responsible for that effect.

Likewise, phosphorylated Smad3 (pSmad3) fluorescence intensity mapping revealed significant down-regulation of canonical (Smadmediated) TGFβ signaling (Fig. 4), suggesting that antifibrotic effects of c8 are due to inhibition of α$_v$β$_1$ integrin–mediated TGFβ activation in vivo.

DISCUSSION

Here, we used a structure-based design to generate the first highly potent and specific inhibitor of the $\alpha_v\beta_1$ integrin. Our results demonstrating a difference of more than five orders of magnitude between concentrations of this inhibitor required to inhibit $\alpha_v\beta_1$ compared to six other integrins that all recognize ligands containing the same arginine–glycine–aspartic acid tripeptide suggest that this reagent is highly selective and should be broadly useful in identifying specific functional roles for $\alpha_v\beta_1$ in vitro and in vivo. Our finding that $\alpha_v\beta_1$ is the major integrin on several different primary fibroblasts responsible for binding to TGFβ_1 LAP and for mediating activation of latent TGFβ by these cells clarifies several previous reports of integrin-mediated TGFβ activation by contractile fibroblasts (17, 24). Our findings that this $\alpha_v\beta_1$-specific small-molecule inhibitor results in the same degree of reversal of liver and lung fibrosis as we previously reported for deletion of all α_v integrins from fibroblasts provide the first convincing evidence that the $\alpha_v\beta_1$ integrin is the major integrin on pathologic fibroblasts responsible for activating latent TGFβ and driving tissue fibrosis in multiple organs. Previous studies have identified expression of $\alpha_v\beta_1$ on a variety of immortalized cell lines, including A549 (23) and human embryonic kidney cells (293 cells) (25), but the ligand or ligands recognized by this integrin have been controversial, and the functional significance of $\alpha_v\beta_1$ has been difficult to determine in the absence of effective and specific inhibitors. $\alpha_v\beta_1$ has thus been alternately described as a receptor for vitronectin (25), fibronectin (8), and the adenovirus penton base (26). One previous study used affinity chromatography of surface-labeled lysates of A549 cells passed over a column composed of recombinant TGFβ_1 LAP cross-linked to Sepharose beads and found that $\alpha_v\beta_1$ could bind to TGFβ_1 LAP, but despite performing coculture TGFβ activity bioassays like the one we used here, the authors could not demonstrate evidence of TGFβ activation (23).

Recent work overexpressing integrin subunits and latent TGFβ in 293 cells also did not demonstrate evidence of TGFβ activation by $\alpha_v\beta_1$ (27). To try to understand the apparent differences between our results and these previous reports, we performed cell adhesion assays and coculture TGFβ bioassays with A549 and 293 cells using the same methods and reagents we used to study CHO cells and fibroblasts (fig. S4). We confirmed that A549 cells adhere well to TGFβ_1 LAP and also found evidence of TGFβ activation. Both effects were potently inhibited by concentrations of c8 as low as 1 nM. However, despite confirming that 293 cells express $\alpha_v\beta_1$, we did not find meaningful adhesion to TGFβ_1 LAP or TGFβ activation by these cells. Future studies examining why 293 cells are incapable of activating TGFβ using this integrin could provide insight into additional mechanisms of regulation of integrin-mediated TGFβ activation.

An important limitation of the current study is that we did not definitively prove that inhibition of TGFβ activation is the only mechanism by which inhibition of $\alpha_v\beta_1$ decreases the magnitude of tissue fibrosis. Although our data suggest that TGFβ activation is one important function of $\alpha_v\beta_1$, it certainly remains possible that other as yet unidentified functions of this integrin also have important effects on tissue fibrosis. The mechanisms that regulate formation and surface expression of the $\alpha_v\beta_1$ heterodimer also need to be identified, because both α_v and β_1 monomers are expressed in nearly every cell, but only a minority of

cells ever express the $\alpha_v\beta_1$ heterodimer on their surface. Finally, our finding that 293 cells can express $\alpha_v\beta_1$ but are incapable of either binding to TGFβ_1 LAP or activating latent TGFβ suggests that there are additional positive and/or negative regulators of the interaction between $\alpha_v\beta_1$ and TGFβ that remain to be identified.

The significant therapeutic effect of our small-molecule $\alpha_v\beta_1$ integrin inhibitor in two different models of fibrotic disease suggest that this integrin could be a promising target for treatment of the multiple chronic diseases characterized by excessive tissue fibrosis. c8 also should be a useful tool to identify additional roles for this understudied member of the integrin family in modulating cell behavior and in vivo biology.

MATERIALS AND METHODS

Study design

The overall goals of this study were to develop and characterize a small-molecule inhibitor of the $\alpha_v\beta_1$ integrin and to assess the possibility that this integrin might be a reasonable therapeutic target for fibrotic diseases affecting multiple organs. To assess the potency and specificity of the candidate inhibitors that we developed, we used in vitro cell adhesion assays and TGFβ activation assays. All in vitro experiments were done at least three times with at least triplicate samples.

To evaluate the potential efficacy of our lead small-molecule c8 in vivo, we compared the effects of c8 to those of the inactive peptide analog c16 in mice treated either with vehicle alone or with the fibrogenic stimuli bleomycin (for induction of pulmonary fibrosis) or CCl_4 (for induction of liver fibrosis). Sample size was selected on the basis of extensive experience with each model to allow us to reliably detect a 50% reduction in the magnitude of fibrosis. Treatments were all delivered by continuous subcutaneous infusion beginning at a time point at which we and others had previously demonstrated that fibrosis was already present. Mice were randomized for inclusion in each of the four treatment arms, and all analyses were performed blind to inciting stimulus and treatment. All surviving mice were included for analysis.

Synthesis of inhibitors

Preparation of ($PhSO_2$)Pro-(pNO_2)Phe-OtBu—Diisopropylethylamine (DIPEA) (1 eq), hydroxybenzotriazole (HOBt) (1 eq), and 1-ethyl-3-(3-dimethylaminopropyl)carbodiimide hydrochloride (EDC•HCl) (1 eq) were added to benzenesulfonylproline (40 mmol) in anhydrous dichloromethane (DCM) (100 ml) at 0 °C, and the solution was stirred for 1 min. Then, nitrophenylalanine *t*-butylester in DCM (300 ml) was added at the same temperature and warmed to room temperature (rt) and stirred overnight. The reaction mixture was washed with 1 N hydrochloric acid (HCl), 10% sodium bicarbonate ($NaHCO_3$), and brine successively. The volatiles were removed under reduced pressure, and the crude product was used without further purification (yellowish foam, 70%). ^{1}H NMR (nuclear magnetic resonance) [dimethylsulfoxide (DMSO)–d_6, 300 MHz] δ ppm 8.4 (1H, s), 8.25 (2H, br s), 7.81-7.57 (7H, m), 4.49 (1H, s), 4.09 (1H, s), 3.34-3.12

(5H, m), 1.58 (3H, br s), and 1.38 (9H, s); LRMS (low-resolution mass spectrometry) [ESI^+ (positive electrospray ionization)] 526.4 (MNa^+).

Preparation of ($PhSO_2$)Pro-(pNH_2)Phe-OtBu—A slurry of Pd/C (palladium on carbon) (0.1 eq based on weight) in MeOH (methanol)/H_2O (1:1, 10 ml) and ammonium formate (9 eq) were added to a solution of the above nitrobenzene (27.9 mmol) in MeOH/THF (tetrahydrofuran) (1:1, 300 ml) at rt. The mixture was heated at 60 °C for 3 hours and cooled to rt. The mixture was filtered through a pad of Celite and concentrated. The crude residue was dissolved in ethyl acetate and washed with saturated $NaHCO_3$ solution, dried over sodium sulfate (Na_2SO_4), and concentrated under reduced pressure. The crude product was used without further purification (off-white foam, 70%). ^{1}HNMR ($CDCl_3$, 300 MHz) δ ppm 7.82 (1H, d, *J* = 9.6 Hz), 7.62-7.53 (3H, m), 7.26-7.22 (1H, m), 6.92 (1H, d, *J* = 10.7 Hz), 6.57 (1H, d, *J* = 10.8Hz), 4.65-4.54 (1H, m), 4.2-4.05 (1H, m), 3.7-3.3 (m, 2H), 3.2-3.0 (2H, m), 2.95-2.85 (1H, m), 2.05 (1H, br s), and 1.6-1.3 (11H, br s); LRMS (ESI^+) 496.2 (MNa^+), 474.5 (MH^+).

Preparation of ($PhSO_2$)Pro-($pNHCOCH_2CH_2CH_2CH_2NHC$= NBocNHBoc)Phe-OtBu—DIPEA (1 eq), HOBt (1 eq), and EDC•HCl (1 eq) were added to the bis-Boc–protected aminopentanoic acid (11.2 mmol) (28) in anhydrous DCM (80 ml) at 0 °C, and then the amine from the previous step (1 eq) in DCM (20 ml) was added at the same temperature, warmed to rt, and stirred overnight. The reaction mixture was washed with 1 N HCl, 10% $NaHCO_3$, and brine successively. The solvent was removed under reduced pressure and purified by silica gel column chromatography (DCM/MeOH, 2% to 5%) to give the off-white foam (74%).

Preparation of c8—The bis-Boc–protected compound prepared from the previous step (8.3 mmol) was treated with 5% anisole in trifluoroacetic acid (TFA) (30 ml) for 3 hours at rt. The volatiles were removed under reduced pressure, and the crude product was washed with diethyl ether several times. The TFA salt was exchanged to chloride using 4 M HCl in dioxane and evaporation under reduced pressure (three times). The final salt was passed through a short pad of silica and dried under reduced pressure. ^{1}H NMR (TFA salt) (300 MHz, DMSO-d_6) ppm δ 9.86 (s, 1H), 8.12 (d, *J* = 7.8 Hz, 1H), 7.81 (d, *J* = 6.9 Hz, 2H), 7.70 (d, *J* = 7.2 Hz, 1H), 7.62–7.15 (m, 7H), 4.41 (s, 1H), 4.15 (s, 1H), 3.33 (s, 1H), 3.1–2.92 (m, 5H), 2.3 (s, 2H), and 1.59–1.48 (m, 8H); LRMS (ESI^+) 559 (MH^+).

Mice

Wild-type C57BL/6 mice were purchased from Jackson Laboratories. Eight- to 12-week-old sex-matched mice were housed under specific pathogen–free conditions in the Animal Barrier Facility of the University of California, San Francisco (UCSF). All experiments were approved by the Institutional Animal Care and Use Committee of the UCSF.

Fibrosis models

Lung and liver fibrosis were induced as described previously (17). In all studies, mice were randomly assigned for each treatment and analyzed in a blinded fashion. For CCl_4-induced liver fibrosis, mice were injected intraperitoneally with sterile CCl_4 (1 μl/g body weight) in a

1:3 ratio with olive oil or olive oil (sham), twice weekly for 6 weeks. Alzet osmotic pumps (Durect) were inserted after 3 weeks of treatment to deliver either c8 or the inactive control small-molecule c16, each dissolved in 50% DMSO (in sterile water) and administered at a dose of 70 mg/kg per day. Livers were harvested 24 hours after the last CCl_4 injection. For bleomycin-induced lung fibrosis, bleomycin (3 U/kg) (Bleo) or water (control) was administered by direct airway intubation with a microsprayer (Penn-Century Inc.). Alzet osmotic pumps were inserted 14 days after treatment as above, and lungs were harvested at 28 days.

Primary cell isolation

Primary murine lung fibroblasts were isolated from 4- to 12-day-old mice using a previously reported method with minor modifications (29). Mouse lungs were removed, pooled together, and digested in an enzyme solution [Hanks' balanced salt solution (without Ca or Mg) with type I collagenase (0.3 mg/ml) (Sigma) and trypsin (0.5 mg/ml) (Sigma)] for 1 hour with removal of dispersed cells every 10 min. Dispersed cells were passed through a sterile filter (70 μm) into Dulbecco's modified Eagle's medium (DMEM)–Ham's F-12 medium (Sigma) and 10% fetal bovine serum, and undigested lung tissue was placed in fresh enzyme solution. Once digestion was complete, erythrocytes were lysed at rt for 10 min using red blood cell lysing buffer (Sigma). Cells were pelleted by centrifugation and cultured in DMEM with 10% fetal bovine serum and 1% penicillin/streptomycin. Nonadherent cells were aspirated and discarded. Primary murine hepatic stellate cells were isolated and passaged as described previously (17). Mouse liver was perfused through the inferior vena cava sequentially with liver perfusion medium (Invitrogen), 0.3% pronase (Roche), and 0.02% collagenase (Sigma). The liver was excised and minced with scissors and further digested in 0.044% pronase and 0.008% deoxyribonuclease (DNase) (Roche). The cell suspension was shaken (200 to 250 rpm) at 37 °C for 10 min and strained through a sterile filter (70 μm). To remove hepatocytes, the cell suspension was centrifuged at 90*g* for 2 min, the supernatant was collected, and DNase was added; this procedure was repeated twice. The supernatant was centrifuged at 700*g* for 7 min to collect the nonparenchymal cell fraction. Collected cells were resuspended in 10 ml of complete DMEM with 10% fetal bovine serum and 1% penicillin/streptomycin and allowed to differentiate in culture into myofibroblasts before use.

Hydroxyproline assay

Mouse lung and liver tissues were homogenized with trichloroacetic acid and incubated overnight at 110 °C in HCl. Samples were reconstituted in water, and hydroxyproline content was measured using the chloramine T assay (30).

IP and Western blotting

Cells were lysed in radioimmunoprecipitation assay buffer [50 mM tris-HCl (pH 7.4), 10 mM $MgCl_2$, 125 mM NaCl, and 2% NP-40]. Cell lysates were centrifuged at 14,000 rpm for 10 min at 4 °C, and the supernatant was collected. Anti-α_v antibody (20 μg) was added to the supernatant, and this was rotated at 4°C for 2 hours, followed by the addition of 30 μl of prewashed protein G–Sepharose slurry (GE Healthcare) for 1 hour at 4 °C. The beads were

washed three times with phosphate-buffered saline (PBS)/protease inhibitor mixture and once with PBS only. Laemmli sample buffer was added, the samples were boiled for 5 min followed by SDS–polyacrylamide gel electrophoresis, and Western blotting was performed. The antibodies that we used for α_v IP were RMV-7 for murine cell lines and L230 for all other cell lines. For α_v Western blotting, we used 611012 (1:500) (BD Biosciences), and for β_1 Western blotting, we used 04-1109 (1:500) (Millipore).

TGFβ activation assay

Test cells were plated at 50,000 cells per well in 96-well plates together with mink lung epithelial cells expressing firefly luciferase downstream of the TGFβ-sensitive portion of the plasminogen activator inhibitor 1 promoter (15,000 to 25,000 cells per well) (22). Cells were cocultured for 16 hours, and TGFβ activity was calculated by measurement of luminescence in the presence and absence of TGFβ-blocking antibody 1D11.

Integrin-specific adhesion assays

The effects of c8 and c16 on cell adhesion mediated by $\alpha_5\beta_1$, $\alpha_8\beta_1$, $\alpha_v\beta_1$, $\alpha_v\beta_3$, $\alpha_v\beta_5$, $\alpha_v\beta_6$, and $\alpha_v\beta_8$ were measured using pairs of cell lines and ligands selected to isolate the effect of each individual integrin. For $\alpha_5\beta_1$, we used the colon carcinoma cell line SW480 plated on fibronectin (0.3 μg/ml); for $\alpha_8\beta_1$, we used SW480 cells transfected with human α_8 adhering to recombinant human TGFβ_1 LAP (1 μg/ml) (31); for $\alpha_v\beta_1$, we used CHOα_v (α_5-deficient CHO cells engineered to express $\alpha_v\beta_1$) adhering to fibronectin (0.3 μg/ml) (8); for $\alpha_v\beta_3$, we used SW480 cells transfected with human β_3 adhering to fibrinogen (1 μg/ml); for $\alpha_v\beta_5$, we used wild-type SW480 cells adhering to vitronectin (0.1 μg/ml); for $\alpha_v\beta_6$, we used SW480 cells transfected with human β_6 adhering to recombinant human TGFβ_1 LAP (0.01 μg/ml); and for $\alpha_v\beta_8$, we used the glioma cell line (SNB19) adhering to recombinant human TGFβ_1 LAP (1 μg/ml). In every case, we confirmed that adhesion could be inhibited by blocking antibodies to the relevant integrin (complex-specific blocking antibodies in all cases except $\alpha_v\beta_1$ for which we showed equivalent effects of blocking α_v). Cells were resuspended in DMEM for 15 to 30 min at 4°C with 10-fold dilutions of c8 with a starting concentration of 10 μM. Each sample was then added to triplicate wells of a 96-well plate that had been coated overnight at 4°C with the relevant ligand, washed with PBS, blocked by 1-hour incubation with 1% bovine serum albumin (BSA), and washed again. Cells were allowed to attach for 60 min at 37°C. After incubation, nonadherent cells were removed by discarding the medium and spinning the plate topside down at 500 rpm for 5 min. Cells were then fixed and stained with 40 μl of 0.5% crystal violet, 1% formaldehyde, 20% MeOH in double-distilled water for 30 min and lysed with 40 μl of 2% Triton-X in PBS. Absorbance was measured at 595 nm in a microplate reader. For all assays, concentration-response curves were constructed by nonlinear regression analysis, and IC_{50} values were calculated using GraphPad Prism software.

Tissue staining

Paraffin-embedded sections were processed as described previously (17). Sections (5 μm) were stained with hematoxylin and eosin or with Sirius red. Pictures were taken from random fields from each section at a final magnification of ×10. Staining area was calculated by pixel counting with National Institutes of Health (NIH) ImageJ. For fluorescence

microscopy, fixed livers and lungs were transferred to 30% sucrose in PBS overnight, embedded in optimum cutting temperature compound, and then cryosectioned at 5 μm. Cryosections were permeabilized and blocked with 0.3% Triton X-100 and 3% BSA in PBS. Sections were incubated with primary antibodies (rabbit anti-pSmad3, Epitomics, 1880-1, 1:100; rat anti-PDGFRβ, eBioscience, 14-1402, 1:100) overnight at 4 °C and then with fluorophore-conjugated secondary antibodies (Invitrogen). Confocal imaging was performed on a Zeiss LSM 5 Pascal microscope. pSmad immunofluorescence staining was quantified as described (32).

Statistical analysis

All results are presented as means ± SEM. Exact *P* values were calculated using the unpaired Student's *t* test for normally distributed data using GraphPad Prism 6.0. *P* values and *n* numbers are shown in the figure legends.

Supplementary Material

Refer to Web version on PubMed Central for supplementary material.

Acknowledgments

We thank E. Wright (University of Michigan) for providing primary human fibroblast from normal lungs and lungs of patients with IPF. We thank R. Juliano (University of North Carolina) for providing integrin α_5–deficient CHO cells. We thank Y. Yokosaki (Hiroshima University) for providing chicken anti-$\alpha_8\beta_1$ antibody. We thank L. Schnapp (University of South Carolina) for providing SW480 cells transfected with human integrin α_8. We thank H. Yagita (Juntendo University) for providing anti-α_V antibody RMV-7. We thank S. Sen from the UCSF Department of Epidemiology and Biostatistics for expert consultation on study design and statistical analysis.

Funding: Financial support was provided by the U.S. NIH grants HL53949 (D.S.), HL108794 (D.S.), and the UCSF Program for Breakthrough Biomedical Research, funded in part by the Sandler Foundation (W.F.D. and D.S.).

Competing interests: N.I.R., H.J., D.S., and W.F.D. are the inventors of the U.S. Patent application no. 61/884,583 related to this work.

REFERENCES AND NOTES

1. Hynes RO. Integrins: Versatility, modulation, and signaling in cell adhesion. Cell. 1992; 69:11–25. [PubMed: 1555235]
2. Munger JS, Sheppard D. Cross talk among TGF-β signaling pathways, integrins, and the extracellular matrix. Cold Spring Harb. Perspect. Biol. 2011; 3:a005017. [PubMed: 21900405]
3. Hynes RO. Integrins: Bidirectional, allosteric signaling machines. Cell. 2002; 110:673–687. [PubMed: 12297042]
4. Sheppard D. In vivo functions of integrins: Lessons from null mutations in mice. Matrix Biol. 2000; 19:203–209. [PubMed: 10936445]
5. Chen C, Sheppard D. Identification and molecular characterization of multiple phenotypes in integrin knockout mice. Methods Enzymol. 2007; 426:291–305. [PubMed: 17697889]
6. Horan GS, Wood S, Ona V, Li DJ, Lukashev ME, Weinreb PH, Simon KJ, Hahm K, Allaire NE, Rinaldi NJ, Goyal J, Feghali-Bostwick CA, Matteson EL, O'Hara C, Lafyatis R, Davis GS, Huang X, Sheppard D, Violette SM. Partial inhibition of integrin αvβ6 prevents pulmonary fibrosis without exacerbating inflammation. Am. J. Respir. Crit. Care Med. 2008; 177:56–65. [PubMed: 17916809]
7. Su G, Hodnett M, Wu N, Atakilit A, Kosinski C, Godzich M, Huang XZ, Kim JK, Frank JA, Matthay MA, Sheppard D, Pittet JF. Integrin αvβ5 regulates lung vascular permeability and

pulmonary endothelial barrier function. Am. J. Respir. Cell Mol. Biol. 2007; 36:377–386. [PubMed: 17079779]

8. Zhang Z, Morla AO, Vuori K, Bauer JS, Juliano RL, Ruoslahti E. The αvβ1 integrin functions as a fibronectin receptor but does not support fibronectin matrix assembly and cell migration on fibronectin. J. Cell Biol. 1993; 122:235–242. [PubMed: 8314844]
9. Munger JS, Huang X, Kawakatsu H, Griffiths MJ, Dalton SL, Wu J, Pittet JF, Kaminski N, Garat C, Matthay MA, Rifkin DB, Sheppard D. The integrin αvβ6 binds and activates latent TGFβ1: A mechanism for regulating pulmonary inflammation and fibrosis. Cell. 1999; 96:319–328. [PubMed: 10025398]
10. Annes JP, Rifkin DB, Munger JS. The integrin $\alpha_v\beta_6$ binds and activates latent TGFβ3. FEBS Lett. 2002; 511:65–68. [PubMed: 11821050]
11. Mu D, Cambier S, Fjellbirkeland L, Baron JL, Munger JS, Kawakatsu H, Sheppard D, Broaddus VC, Nishimura SL. The integrin αvβ8 mediates epithelial homeostasis through MT1-MMP-dependent activation of TGF-β1. J. Cell Biol. 2002; 157:493–507. [PubMed: 11970960]
12. Aluwihare P, Mu Z, Zhao Z, Yu D, Weinreb PH, Horan GS, Violette SM, Munger JS. Mice that lack activity of αvβ6- and avβ8-integrins reproduce the abnormalities of *Tgfb1*- and *Tgfb3*-null mice. J. Cell Sci. 2009; 122:227–232. [PubMed: 19118215]
13. Minagawa S, Lou J, Seed RI, Cormier A, Wu S, Cheng Y, Murray L, Tsui P, Connor J, Herbst R, Govaerts C, Barker T, Cambier S, Yanagisawa H, Goodsell A, Hashimoto M, Brand OJ, Cheng R, Ma R, McKnelly KJ, Wen W, Hill A, Jablons D, Wolters P, Kitamura H, Araya J, Barczak AJ, Erle DJ, Reichardt LF, Marks JD, Baron JL, Nishimura SL. Selective targeting of TGF-β activation to treat fibroinflammatory airway disease. Sci. Transl. Med. 2014; 6:241ra79.
14. Ma LJ, Yang H, Gaspert A, Carlesso G, Barty MM, Davidson JM, Sheppard D, Fogo AB. Transforming growth factor-β-dependent and -independent pathways of induction of tubulo-interstitial fibrosis in $\beta6^{-/-}$ mice. Am. J. Pathol. 2003; 163:1261–1273. [PubMed: 14507636]
15. Melton AC, Bailey-Bucktrout SL, Travis MA, Fife BT, Bluestone JA, Sheppard D. Expression of αvβ8 integrin on dendritic cells regulates Th17 cell development and experimental autoimmune encephalomyelitis in mice. J. Clin. Invest. 2010; 120:4436–4444. [PubMed: 21099117]
16. Kudo M, Melton AC, Chen C, Engler MB, Huang KE, Ren X, Wang Y, Bernstein X, Li JT, Atabai K, Huang X, Sheppard D. IL-17A produced by αβ T cells drives airway hyper-responsiveness in mice and enhances mouse and human airway smooth muscle contraction. Nat. Med. 2012; 18:547–554. [PubMed: 22388091]
17. Henderson NC, Arnold TD, Katamura Y, Giacomini MM, Rodriguez JD, McCarty JH, Pellicoro A, Raschperger E, Betsholtz C, Ruminski PG, Griggs DW, Prinsen MJ, Maher JJ, Iredale JP, Lacy-Hulbert A, Adams RH, Sheppard D. Targeting of α_V integrin identifies a core molecular pathway that regulates fibrosis in several organs. Nat. Med. 2013; 19:1617–1624. [PubMed: 24216753]
18. Nagae M, Re S, Mihara E, Nogi T, Sugita Y, Takagi J. Crystal structure of α5β1 integrin ectodomain: Atomic details of the fibronectin receptor. J. Cell Biol. 2012; 197:131–140. [PubMed: 22451694]
19. Xiong JP, Stehle T, Zhang R, Joachimiak A, Frech M, Goodman SL, Arnaout MA. Crystal structure of the extracellular segment of integrin αVβ3 in complex with an Arg-Gly-Asp ligand. Science. 2002; 296:151–155. [PubMed: 11884718]
20. Miller MW, Basra S, Kulp DW, Billings PC, Choi S, Beavers MP, McCarty OJ, Zou Z, Kahn ML, Bennett JS, DeGrado WF. Small-molecule inhibitors of integrin $\alpha_2\beta_1$ that prevent pathological thrombus formation via an allosteric mechanism. Proc. Natl. Acad. Sci. U.S.A. 2009; 106:719–724. [PubMed: 19141632]
21. Shi M, Zhu J, Wang R, Chen X, Mi L, Walz T, Springer TA. Latent TGF-β structure and activation. Nature. 2011; 474:343–349. [PubMed: 21677751]
22. Abe M, Harpel JG, Metz CN, Nunes I, Loskutoff DJ, Rifkin DB. An assay for transforming growth factor-β using cells transfected with a plasminogen activator inhibitor-1 promoter-luciferase construct. Anal. Biochem. 1994; 216:276–284. [PubMed: 8179182]
23. Munger JS, Harpel JG, Giancotti FG, Rifkin DB. Interactions between growth factors and integrins: Latent forms of transforming growth factor-β are ligands for the integrin αvβ1. Mol. Biol. Cell. 1998; 9:2627–2638. [PubMed: 9725916]

24. Wipff PJ, Rifkin DB, Meister JJ, Hinz B. Myofibroblast contraction activates latent TGF-β1 from the extracellular matrix. J. Cell Biol. 2007; 179:1311–1323. [PubMed: 18086923]
25. Bodary SC, McLean JW. The integrin β_1 subunit associates with the vitronectin receptor α_v subunit to form a novel vitronectin receptor in a human embryonic kidney cell line. J. Biol. Chem. 1990; 265:5938–5941. [PubMed: 1690718]
26. Li E, Brown SL, Stupack DG, Puente XS, Cheresh DA, Nemerow GR. Integrin αvβ1 is an adenovirus coreceptor. J. Virol. 2001; 75:5405–5409. [PubMed: 11333925]
27. Dong X, Hudson NE, Lu C, Springer TA. Structural determinants of integrin β-subunit specificity for latent TGF-β. Nat. Struct. Mol. Biol. 2014; 21:1091–1096. [PubMed: 25383667]
28. Choi S, Isaacs A, Clements D, Liu D, Kim H, Scott RW, Winkler JD, DeGrado WF. De novo design and in vivo activity of conformationally restrained antimicrobial arylamide foldamers. Proc. Natl. Acad. Sci. U.S.A. 2009; 106:6968–6973. [PubMed: 19359494]
29. Bruce MC, Honaker CE, Cross RJ. Lung fibroblasts undergo apoptosis following alveolarization. Am. J. Respir. Cell Mol. Biol. 1999; 20:228–236. [PubMed: 9922213]
30. Reddy GK, Enwemeka CS. A simplified method for the analysis of hydroxyproline in biological tissues. Clin. Biochem. 1996; 29:225–229. [PubMed: 8740508]
31. Lu M, Munger JS, Steadele M, Busald C, Tellier M, Schnapp LM. Integrin α8β1 mediates adhesion to LAP-TGFβ1. J. Cell Sci. 2002; 115:4641–4648. [PubMed: 12415008]
32. Arnold TD, Ferrero GM, Qiu H, Phan IT, Akhurst RJ, Huang EJ, Reichardt LF. Defective retinal vascular endothelial cell development as a consequence of impaired integrin αVβ8-mediated activation of transforming growth factor-β. J. Neurosci. 2012; 32:1197–1206. [PubMed: 22279205]

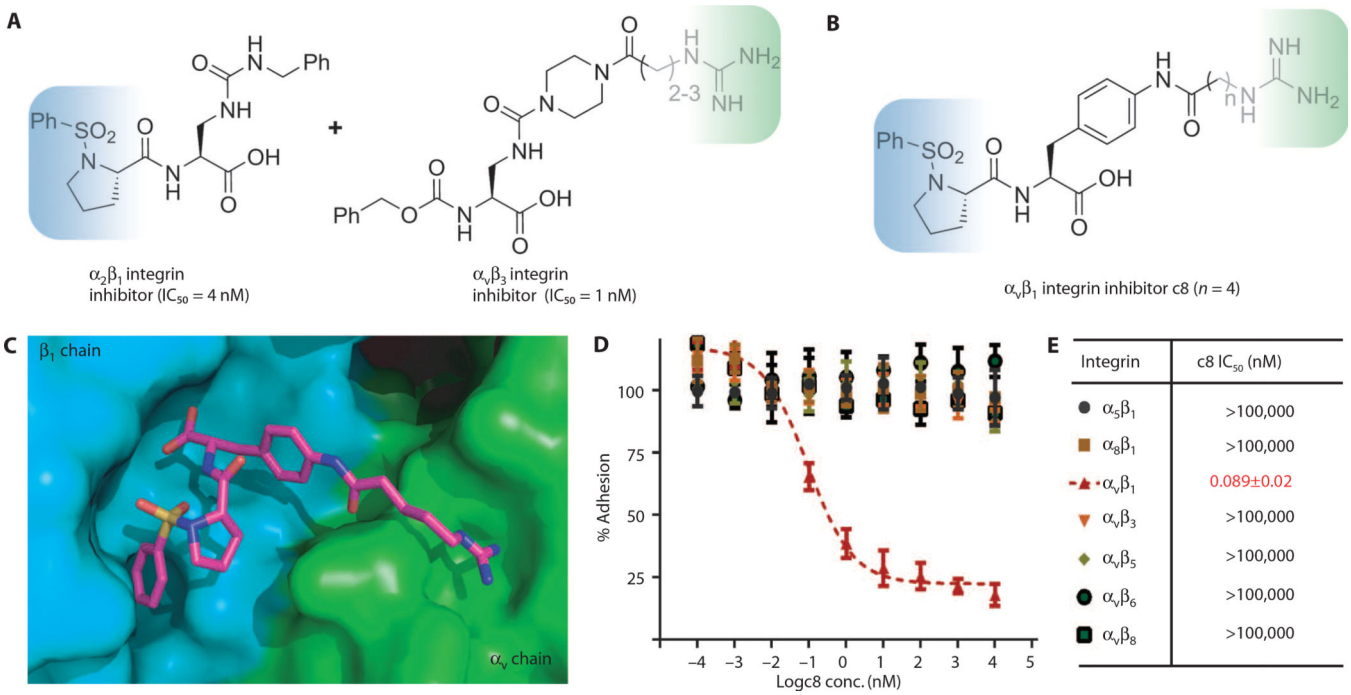

Fig. 1. $\alpha_v\beta_1$ integrin inhibitor design and demonstration of potency and specificity

(**A**) Design principle of $\alpha_v\beta_1$ integrin inhibitor by combining a positively charged guanidine moiety in $\alpha_v\beta_3$ integrin inhibitor (blue shading) and a sulfonamidoproline moiety in $\alpha_2\beta_1$ integrin inhibitor (green shading). (**B**) Structures of $\alpha_v\beta_1$ integrin–specific inhibitor c8. (**C**) Docking model of $\alpha_v\beta_1$ integrin inhibitor c8 bound to $\alpha_v\beta_1$ integrin, where α and β subunits are, respectively, in green and blue. The model predicted that a linker length of $n = 3$ or 4 would have the highest affinity. (**D**) Dose-dependent cell adhesion assay of c8 against all α_v and related integrins. (**E**) Curve-fitted IC_{50} of c8 against RGD (arginine–glycine– aspartic acid)–binding integrins in cell adhesion assay. Data represent means ± SEM; $n = 3$ (three experimental replicates).

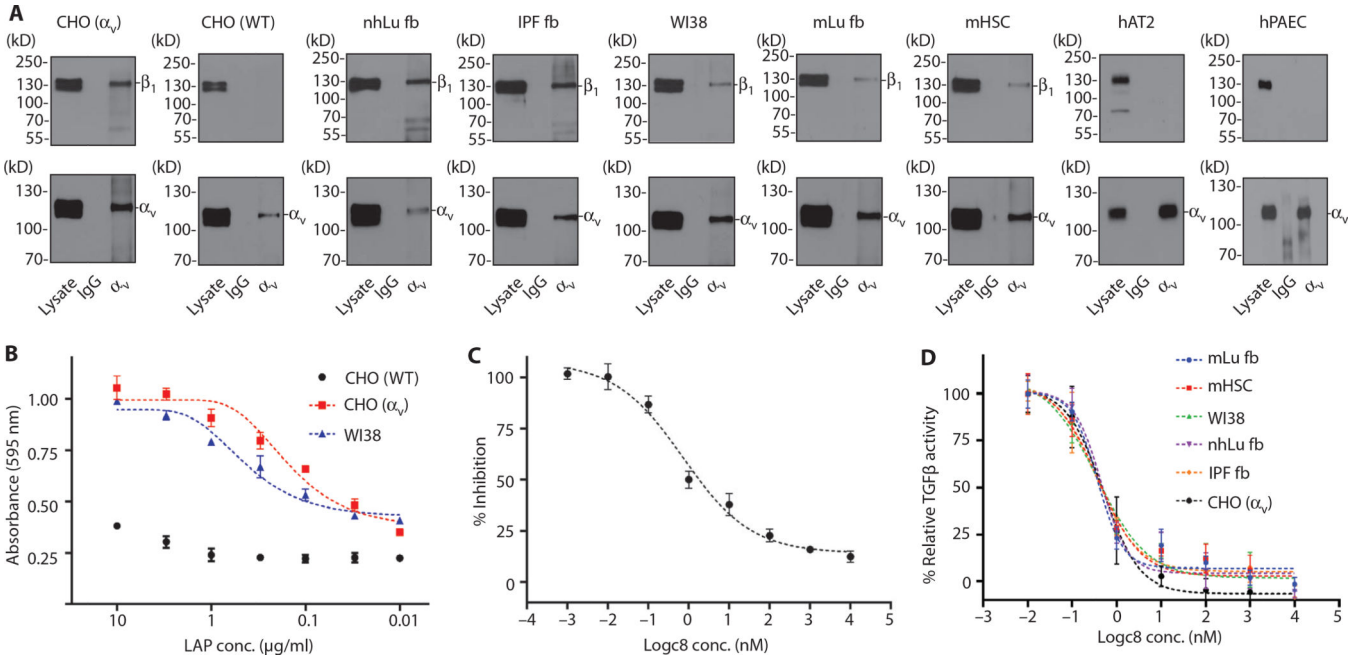

Fig. 2. $\alpha_v\beta_1$ is expressed on pulmonary and hepatic fibroblasts and mediates adhesion to TGFβ_1 LAP and activation of latent TGFβ

(**A**) Coimmunoprecipitation and Western blot reveal expression of $\alpha_v\beta_1$ heterodimers in human and murine cell lines from the liver and lung. Cell lysates were immunoprecipated with antibodies to α_v (antibody RMV-7 for murine cells or L230 for all other cells), followed by Western blotting for either α_v (lower panels, to control for capture, antibody 611012) or β_1 (upper panels, antibody 04-1109). nhLu fb control (normal human lung fibroblasts from an uninjured control subject); IPF fb (lung fibroblasts isolated from a patient with IPF); mLu fb (murine lung fibroblasts); mHSC (murine hepatic stellate cells); WI38 (diploid human lung fibroblast); CHO [WT (wild-type)] control α_5-deficient CHO cells (which lack expression of $\alpha_v\beta_1$); CHO (α_v) (α_5-deficient CHO cells engineered to express the $\alpha_v\beta_1$); hAT2 (human alveolar type 2 cells, which lack expression of $\alpha_v\beta_1$); hPAEC (human pulmonary artery endothelial cells, which lack expression of $\alpha_v\beta_1$). IgG, immunoglobulin G. (**B**) WT CHO cells (lacking $\alpha_v\beta_1$) adhere poorly, whereas CHO cells with forced expression of $\alpha_v\beta_1$ (CHO α_v) and WI38 cells strongly adhere to TGFβ_1 LAP. (**C**) WI38 cell adhesion to TGFβ_1 LAP (0.3 μg/ml) is inhibited by c8 (IC_{50} = 0.72 nM). (**D**) c8 treatment reduced activation of TGFβ by cells expressing $\alpha_v\beta_1$ (IC_{50} range, 0.35 to 0.50nM). Fibroblasts (as indicated) were cocultured with TGFβ reporter (PAI1-luciferase) cell line in the presence of a range of concentrations of c8. Data represent means ± SEM, *n* = 3 (three experimental replicates).

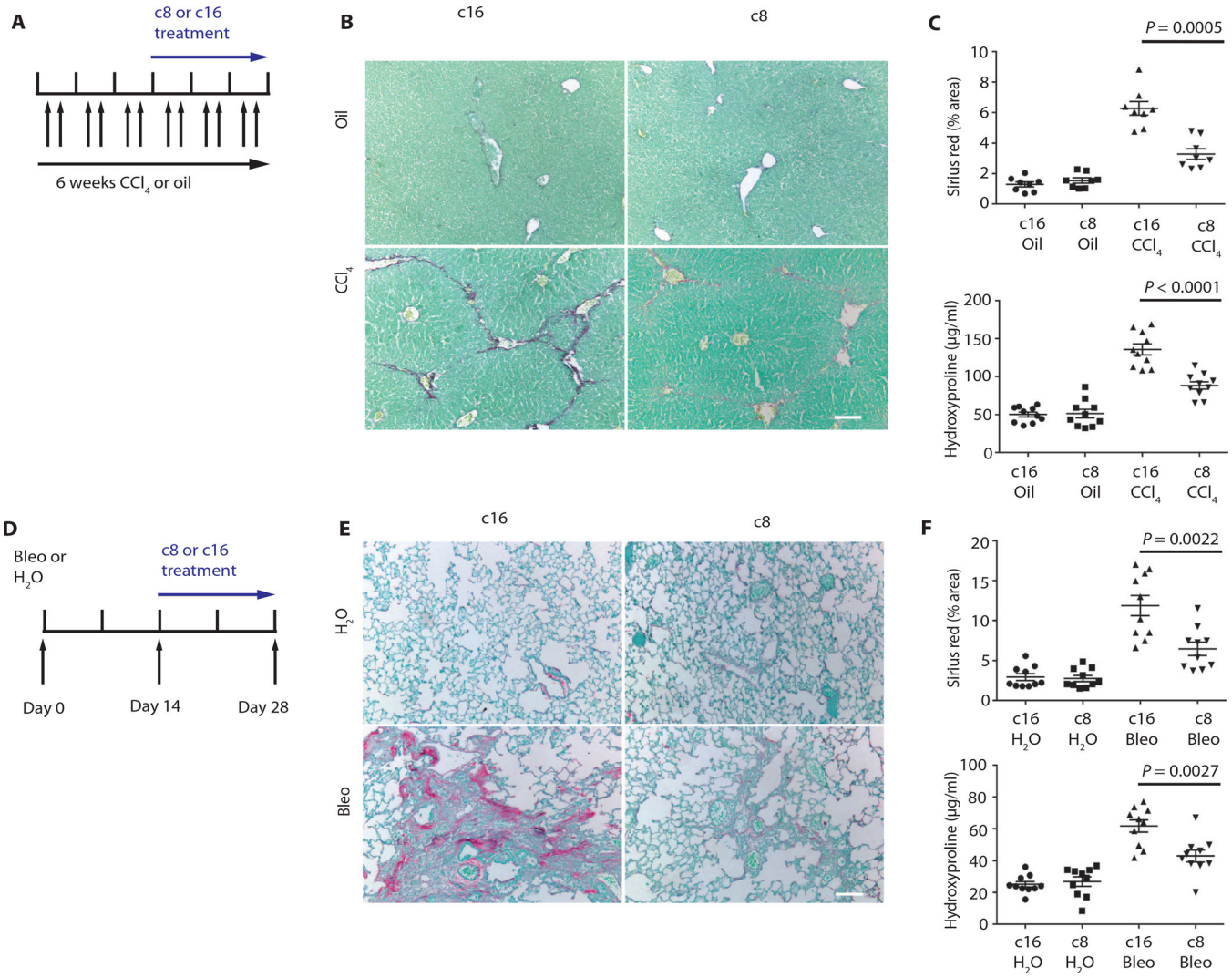

Fig. 3. c8 protects from liver and lung fibrosis

(**A**) Effects of c8 or c16 on mouse fibrosis model (liver). c8 or c16 (inactive control compound) was continuously delivered by Alzet pump beginning 3 weeks after intraperitoneal administration with oil (sham) or CCl_4 to induce liver fibrosis. (**B** and **C**) Treatment with c8 significantly reduced liver fibrosis, as determined by (B) Sirius red staining (collagen deposition) of liver tissue after olive oil (top panels) or CCl_4 treatment (bottom panels), (C) digital image analysis quantification of collagen staining, and hydroxyproline analysis. Sirius red (liver) $n = 8$; $P = 0.0005$. Hydroxyproline (liver) $n = 10$; $P < 0.0001$. (**D**) Effects of c8 or c16 on murine fibrosis model (lung). c8 or c16 was continuously delivered to mice using Alzet pumps beginning 14 days after intratracheal instillation of bleomycin (Bleo) to induce pulmonary fibrosis or water (H_2O). (**E** and **F**) Treatment with c8 significantly reduced lung fibrosis, as determined by (E) Sirius red staining (collagen deposition) of lung tissue after water (top panels) or bleomycin treatment (bottom panels), (F) digital image analysis quantification of collagen staining, and hydroxyproline analysis. Sirius red (lung) $n = 10$; $P = 0.0022$. Hydroxyproline (lung) $n = 10$;

$P = 0.0027$. Data represent means ± SEM. Scale bars, 100 μm. *P* values were calculated using the unpaired Student's *t* tests.

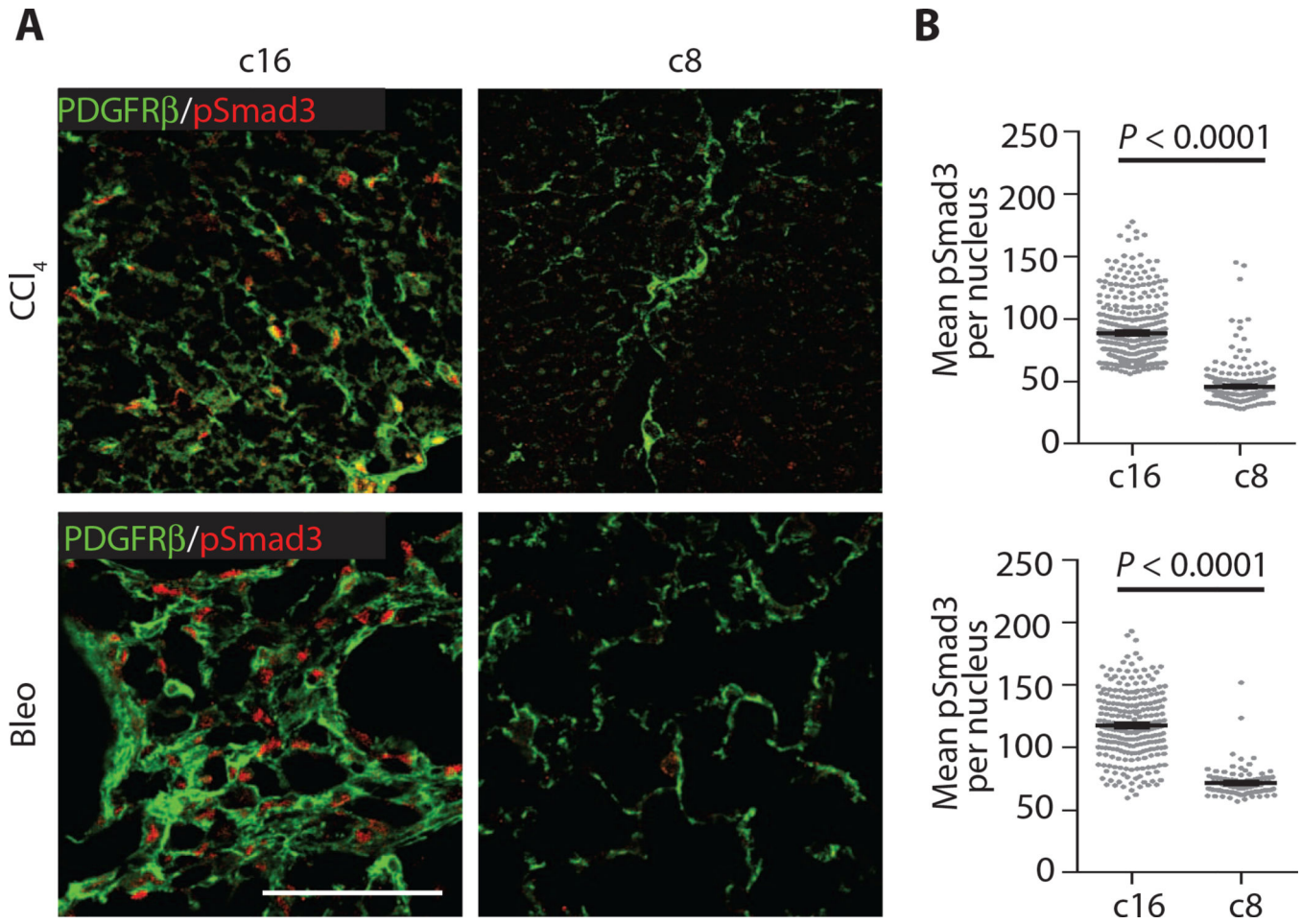

Fig. 4. Reduced pSmad3 in mice treated with c8

(**A**) Representative liver (top panels) and lung (bottom panels) sections from mice treated with c16 or c8 after induced fibrotic injury stained for fibroblasts [PDGFRβ (plateletderived growth factor receptor β), green] and pSmad3 (red). (**B**) Quantification of pSmad3 nuclear intensity within individual PDGFRβ$^+$ cells documents a significant reduction in fibroblast-specific pSmad3 in fibrotic mice treated with c8. Data represent means ± SEM; $n = 102$ (Bleo c8), $n = 254$ (Bleo c16), $n = 262$ (CCl_4 c8), and $n = 361$(CCl_4 c16). For both comparisons, $P < 0.0001$ (shown is a representative example of the distribution of individual pSmad3 mean fluorescence intensities in PDGFRβ$^+$ cells, and the average of these means, for a single sample condition). Scale bar, 100 μm. *P* values were calculated using the unpaired Student's *t* tests.